Uncoupling of Electron and Proton Transfers in the Photocycle of Bacterial Reaction Centers under High Light Intensity †

ARTICLE *in* BIOCHEMISTRY · MAY 2006

Impact Factor: 3.02 · DOI: 10.1021/bi052071m · Source: PubMed

Uncoupling of Electron and Proton Transfers in the Photocycle of Bacterial Reaction Centers under High Light Intensity†

László Gerencsér and Péter Maróti*

Department of Biophysics, University of Szeged, Egyetem utca 2, Szeged, Hungary H-6722

Received October 11, 2005; Revised Manuscript Received February 10, 2006

ABSTRACT: Photosynthetic reaction centers produce and export oxidizing and reducing equivalents in expense of absorbed light energy. The formation of fully reduced quinone (quinol) requires a strict (1:1) stoichiometric ratio between the electrons and H^+ ions entering the protein. The steady-state rates of both transports were measured separately under continuous illumination in the reaction center from the photosynthetic bacterium *Rhodobacter sphaeroides*. The uptake of the first proton was retarded by different methods and made the rate-limiting reaction in the photocycle. As expected, the rate constant of the observed proton binding remained constant (7 s^{-1}), but that of the cytochrome photooxidation did show a remarkably large increase from 14 to 136 s^{-1} upon increase of the exciting light intensity up to 5 W/cm^2 (808 nm) at pH 8.4 in the presence of $NiCl_2$. This corresponds to about 20:1 (e^-:H^+) stoichiometric ratio. The observed enhancement is linearly proportional to the light intensity and the rate constant of the proton uptake by the acceptor complex and shows saturation character with quinone availability. For interpretation of the acceleration of cytochrome turnover, an extended model of the photocycle is proposed. A fraction of photochemically trapped RC can undergo fast (>10^3 s^{-1}) conformational change where the semiquinone loses its high binding affinity (the dissociation constant increases by more than 5 orders of magnitude) and dissociates from the Q_B binding site of the protein with a high rate of 4000 s^{-1}. Concomitantly, superoxide is being produced. No H^+ ion is taken up, and no quinol is created by the photocycle which is operating in about 25% of the reaction centers at the highest light intensity (5500 s^{-1}) and slowest proton uptake (3.5 s^{-1}) used in our experiments. The possible physical background of the light-induced conformational change and the relationship between the energies of dissociation and redox changes of the quinone in the Q_B binding sites are discussed.

The reaction center (RC)[1] of photosynthetic bacteria is a membrane-bound pigment protein complex that couples light-induced electron transfer to the first steps of vectorial proton transfer across the bacterial membrane (*1*−*3*). The electrons come from the photoexcited bacteriochlorophyll dimer (P*) and the protons from the cytoplasmic side via quinol production: $Q + 2e^- + 2H^+ \rightarrow QH_2$. Unlike other well-known proton pumps, such as cytochrome oxidase (*4*) and bacteriorhodopsin (*5*), the transmembrane proton translocation is completed in cooperation with an additional membrane protein, the cytochrome bc_1 complex that reoxidizes the quinol (*6*). The transmembrane proton gradient serves as the ultimate free energy source of the organism to drive energy-consuming reactions such as ion transport and ATP synthesis (*7*, *8*). The ATP fills the majority of the energy needs of the bacterium.

The RC from the bacterium *Rhodobacter sphaeroides* consists of three subunits, L, M, and H, and 10 cofactors (*9*). The LM dimer binds all of the cofactors arranged around a quasi-2-fold rotational symmetry axis. The H subunit caps the LM dimer and stabilizes both the structure of the protein and the function of the quinones (*10*). The light-induced electron transfer proceeds along the A branch from the excited singlet state of P through a bacteriochlorophyll

† Financial support from the OTKA (TO42680), Balaton (F-4/04), and MTA-CNR to P.M. and the Bolyai fellowship to L.G. is gratefully acknowledged.

* To whom correspondence should be addressed. Tel: 36-62-544-120. Fax: 36-62-544-121. E-mail: pmaroti@sol.cc.u-szeged.hu.

[1] Abbreviations: Bpheo, bacteriopheophytin; CT, conformational transition; cyt c^{3+} and cyt c^{2+}, oxidized and reduced cytochrome *c*, respectively; E_h, actual redox potential; E_m, midpoint redox potential at pH 7; *I*, light intensity of excitation measured in % or in W/cm^2 (100% corresponds to $k_P = 5500$ s^{-1}); I_{50}, apparent inhibition constant; In, inhibitor; k_BT, Boltzmann factor; k_c, effective rate constant of cytochrome oxidation by P^+ and exchange for a reduced cytochrome from the pool; k_{cyt}, observed rate constant of cytochrome photooxidation; k_H, rate constant of the first proton uptake $Q_A^-Q_B^- + H^+ \rightarrow Q_A^-Q_B(H)$; k_H(obs), rate constant of observed proton binding during continuous excitation; k_{off}, rate constant of dissociation; k_{on}, bimolecular rate constant of association; k_p, rate constant of the $PQ_A \rightarrow P^+Q_A^-$ photochemical reaction; k_{QH_2}, rate constant of quinol formation; k_+ and k_-, forward and backward rate constants of conformational change, respectively; K_2, one-electron equilibrium constant in the quinone complex; $K_{conf} = k_+/k_-$, equilibrium constant of conformational change; $K_D = k_{off}/k_{on}$, dissociation equilibrium constant; LDAO, *N*,*N*′-dimethyldodecylamine *N*-oxide; MES, 2-(*N*-morpholino)ethanesulfonic acid; MOPS, 3-(*N*-morpholino)propanesulfonic acid; NBT, nitrotetrazolium blue chloride (nitroblue tetrazolium); NQ, naphthoquinone; P (P^+), reduced (oxidized) bacteriochlorophyll dimer; Q (Q^-), oxidized (reduced) quinone; Q_A and Q_B, primary and secondary quinone, respectively; QH_2, dihydroquinone (quinol); *Rb*., *Rhodobacter*; RC, reaction center protein; SOD, superoxide dismutase; TMPD, *N*,*N*,*N*′,*N*′-tetramethyl-1,4-phenylenediamine; Tris, 2-amino-2-(hydroxymethyl)propane-1,3-diol; Triton X-100, polyoxyethylene(10) isooctylphenyl ether; UQ_0, 2,3-dimethoxy-5-methylbenzoquinone; UQ_6, ubiquinone-30; UQ_{10}, ubiquinone-50.

10.1021/bi052071m CCC: $33.50
Published on Web 04/07/2006

monomer and a bacteriopheophytin monomer (Bpheo). From $Bpheo^-$, the electron is transferred within 200 ps to the primary quinone (Q_A), and the Q_A^- reduces directly or indirectly the secondary quinone Q_B in 100 μs (*11*). The two quinones constitute a functional acceptor quinone complex. Although they are chemically identical species (ubiquinones), their physical−chemical (electrochemical) properties are different due to their interaction with the protein (*2*, *3*, *12*). While Q_A makes one-electron chemistry, Q_B can perform full reduction with two electrons and two protons (two-electron gate mechanism). All cofactors are tightly bound except for Q_B, which is in weak binding equilibrium when oxidized (Q_B) or fully reduced (Q_BH_2). However, when reduced with one electron to Q_B^-, it is tightly bound (*13*, *14*).

In the presence of an external electron donor (cytochrome c_2 in vivo), P^+ is rereduced by reduced cytochrome *c* (cyt $c^{2+} + P^+ \rightarrow$ cyt $c^{3+} + P$), and the RC in $PQ_AQ_B^-$ state can undergo another light-driven reaction. After a new (second) excitation of P, $P^+Q_A^-Q_B^-$ is formed. Sequential and alternative electron transfer and proton uptake steps lead to full reduction of Q_B to quinol (dihydroquinone) Q_BH_2: after uptake of the first proton, Q_BH is formed from Q_B^-, followed by the second reduction, Q_BH^-, and finally by the uptake of the second proton (*15*). Two light reactions oxidize two cytochromes and reduce one quinone. The quinol leaves the RC and is replaced by an oxidized quinone from the membrane quinone pool (*16*). The return of the acceptor quinone system to its original state allows the turnover of RC under multiple-flash activation or continuous illumination. The binary oscillations of semiquinone (*17*) and proton uptake from the aqueous phase (*18*) as responses to repetitive flash excitation or the accumulation of photooxidized cytochromes under continuous illumination (*19*−*21*) have become routine tools to study RC function. These assays are very sensitive to slight modifications of the supply and coupling of electrons and protons in the donor and acceptor sides of the RC due to mutations, inhibitions, or structural changes.

According to the sequence of events summarized as the acceptor quinone reduction cycle, the coupling between the electron transfer and the proton uptake is strong. This is expressed by the simple correlation between the rate of photooxidation of cytochrome (k_{cyt}) and the rate of the quinol formation (k_{QH_2}) (or the turnover rate of the RC): $k_{cyt} = 2k_{QH_2}$. As the photocycle consists of many steps, its rate depends on the rates of its constituents on a complex way but cannot be larger than the rate of the slowest process. The observed rate of cytochrome photooxidation reflects the bottleneck of the quinone reduction cycle that can accommodate to the physiological conditions. Under moderate intensity of illumination, when the frequency of RC excitation is much less than 10^3 s^{-1}, the light intensity is the rate-limiting factor, as the electron and proton transfers and exchange (binding and unbinding) processes ($k_{on} + k_{off}$) on the donor (cyt c^{3+}/cyt c^{2+}) and acceptor (quinone/quinol) sides are faster than 10^3 s^{-1}. However, the rate-limiting role of the slowest step can be easily shifted to any other reactions if they become slower (mainly due to depletion of the cytochrome or quinone pools under continuous operation or inhibition of the proton uptake/electron transfer) and/or the light intensity (or the efficiency of harvesting the light) increases. Under well-controlled conditions, the slowest step can be identified (*20*, *21*).

If the focus of interest is on the coupling of electron transfer and proton uptake in RC, high light intensity should be used to avoid its rate limitation in the photocycle. The kinetic step of the proton uptake can be easily made as a bottleneck of the photocycle by binding of several divalent transition metal ions to the surface histidines (H126 and H128) and to one of the two aspartic acid residues (H124 or M17) at the entry point of the proton delivery channel (*22*−*25*). The rate of the inhibited second interquinone electron transfer is not sensitive to changes of the electron transfer driving force; therefore, the observed kinetics are clearly limited by the proton transfer (*23*). Under these conditions, the rate of the cytochrome photooxidation should not depend on the light intensity. Contrary to this expectation, the rate did show light intensity dependence indicating the contribution of reactions not involved in the simple scheme of the quinone reduction cycle.

In this work, we investigated the structural and functional aspects of this novel observation, called acceleration of cytochrome photooxidation in RC with retarded acceptor quinone function. The steep increase of the rate of the photooxidation of cytochrome vs light intensity was not accompanied with increase in proton uptake or quinol formation. The less tight coupling between the electron and proton transfers is attributed to light-induced changes in protein conformation that makes the Q_B^- semiquinone anion less stable in the binding pocket. Consequently, it dissociates from the RC before proton binding and makes the cytochrome oxidation (electron transfer) more effective than the uptake of H^+ ions (proton transfer). The kinetic and thermodynamic details of the mismatch in the coupling will be discussed. Preliminary accounts of this work have been presented (*26*).

MATERIALS AND METHODS

Materials. Ubiquinone UQ_6 and UQ_0 (Sigma) were solubilized in ethanol in stock solutions of 1 and 500 mM, respectively. The UQ_{10} (Sigma) was sonicated in detergent of Triton X-100 (30% w/v). The antibiotic stigmatellin (Fluka) and triazine-type terbutryn (Chem Service) were solubilized in ethanol in stock solution of 5 and 60 mM, respectively. Mammalian (horse heart) cytochrome *c* (Sigma, type VI) was reduced (>95%) by adding sodium ascorbate to its solution and was separated from sodium ascorbate by chromatography on Sephadex G-25 (Pharmacia) or by bubbling H_2 gas through its solution in the presence of palladium black (Aldrich). The concentration of reduced cyt *c* was obtained using an extinction coefficient of ϵ_{550}(reduced) = 27.6 $mM^{-1}\cdot cm^{-1}$ (*27*). The quantity of accumulated photooxidized cytochrome *c* was calibrated on the basis of the difference extinction coefficient of ϵ_{550}(reduced) − ϵ_{550}(oxidized) = 21.1 $mM^{-1}\cdot cm^{-1}$ (*28*). The water-soluble TMPD (Sigma) was reduced by addition of sodium ascorbate prior to use. Ferrocene (Sigma) was dissolved in ethanol and used after preparation without further reduction, as its redox midpoint potential is relatively high [E_m(ferrocene/ferrocenium) ≈ 400 mV; unpublished data]. The pH-indicator absorption dye, *o*-cresol red (Sigma) was dissolved in ethanol and used in a concentration of 30 μM, which was the optimum selection to ensure a fast and saturating response

of the dye and to keep the absorption of the sample low. Detergents LDAO and Triton X-100 and buffers (MES, MOPS, Tris) were obtained from Fluka and Sigma, respectively. The aliquots of hydrochloric acid (HCl) were prepared from 0.1 M stock solution (Fisher). All materials were used without any further purification.

Reaction Center. RCs were isolated from the blue-green (carotenoidless) mutant (strain R-26) of the photosynthetic bacterium *Rb. sphaeroides* as described earlier (*18*). The zwitterionic detergent (LDAO) was changed for nonionic detergent (Triton X-100) by overnight dialysis against 1 mM Tris buffer (pH 8) at 4 °C. The OD(280 nm)/OD(802 nm) ratio, a measure of the purity of the RC, was smaller than 1.40. The secondary quinone activity [the ratio of the amplitudes of the kinetic phases of the charge recombination (*29*)] dropped to 10% during the preparation. The concentration of the RC was determined from the steady-state absorption at 802 nm ($\epsilon = 288$ $mM^{-1}\cdot cm^{-1}$) or from the absorption change at 430 nm ($\Delta\epsilon = 26$ $mM^{-1}\cdot cm^{-1}$) induced by continuous laser light (*21*).

Chromatophore. The chromatophore was isolated from the cytochrome c_2-less mutant of *Rb. sphaeroides* (Cyca1, a generous gift of Prof. C. A. Wraight). Similar mutant was used by Lavergne et al. (*30*). The concentration of the RC in the chromatophore suspension was determined from the flash-induced absorption change at 603 nm using the difference extinction coefficient of 20 $mM^{-1}\cdot cm^{-1}$ and was adjusted routinely to 0.1 μM.

Optical Measurements. Steady-state absorption spectra were recorded with a Unicam UV4 spectrophotometer. Kinetic measurements were made with a single-beam spectrophotometer of local design (*18*, *21*, *31*). Saturating flashes were produced by a Xe flash tube (FX-200 EG/G) with red filter. Continuous actinic illumination was provided by a laser diode (High Power Devices, Inc., type 1010, emission wavelength 808 nm, maximum power 1 W) controlled by a homemade driver (the operating current was stabilized at 1.2 A). The duration and intensity of the laser emission were adjusted by a digital pulse generator (Híradástechnika, type TR 0360), and the rectangularity of the shape of the laser emission was checked by the combination of a photodiode and an oscilloscope. The rise and fall times were below 1 μs, and the slope of the constant part was less than 5%. The focused measuring beam was within the laser excited area (0.2 cm^2) of the 3 × 3 mm rectangular quartz cuvette held in a massive brass block.

The rate of the primary photochemistry was determined from the monoexponential rise of P^+ detected at 865 nm that was generated by continuous illumination in the absence of an electron donor to P^+. The sample containing reduced cytochrome was prepared in full darkness and was thermostated at room temperature (23 °C). After photooxidation of the cytochromes, the sample was discarded, and new RC was taken for the next illumination. In all experiments, the concentration of the RC was selected to 1 μM to keep the internal screening (attenuation) of the exciting light constant. In this way, the same relationship between the light intensity (I) and the rate constant of the primary photochemistry (k_p) could be used throughout the work.

Measurement of Proton Uptake. The pH indicator dye *o*-cresol red was used to follow the pH change of the solution due to light-induced protonation of the RC. The buffering capacity of the RC solution was decreased by overnight dialysis against a solution of 10 μM Tris, 0.03% Triton X-100, and 50 mM NaCl at pH 8.0. The cytochrome *c* was replaced by ferrocene. Although the ferrocene is a slower donor to P^+ than cyt c^{2+}, its redox change is not accompanied with protonation and has negligible absorption change upon oxidation at the wavelength (572 nm) of the maximal sensitivity of the *o*-cresol red. The net proton binding was obtained by subtracting the signal of the buffered sample (10 mM Tris) from that of the dye response. The calibration occurred by addition (mixing) of a known amount of HCl to the solution (*18*, *32*).

Assay for Superoxide Synthesis. The formation of superoxide and its subsequent reactions were detected by two conventional spectrophotometric methods: (1) reduction of nitroblue tetrazolium (Sigma, N6876) (*33*) and (2) reduction of oxidized cytochrome (*34*) whose reaction can be inhibited by superoxide dismutase (Sigma, EC 1.15.1.1). On the basis of the NBT assay for superoxide synthesis, the quantity of escaped electrons by dissociation of the semiquinone from the RC could be determined. To calculate the specific activity, the reduction of the yellow, water-soluble NBT to blue, water-insoluble diformazan by superoxide radicals was monitored by the increase in absorbance at 530 nm, using 12.8 $mM^{-1}\cdot cm^{-1}$ as the extinction coefficient (*35*). For cytochrome assay of the superoxide, the reduced (>95%) cytochrome pool was partially oxidized by O_2 in the dark, and then the reaction between the superoxide radical and oxidized cytochrome was followed spectrophotometrically at 550 nm in the absence and presence of active and inactive SOD. SOD was denatured by heating at 95 °C for 1 h (*36*).

Fitting Procedures. The kinetic traces were recorded by a digital oscilloscope (Hitachi VC-6025) interfaced with an IBM computer system of local design. Changes in optical transmission were converted to units of absorption, and the kinetic analysis of the absorption transients was performed by nonlinear least-squares fitting according to the Levenberg−Marquardt algorithm. Model calculations were carried out using Mathcad 4.0.

RESULTS

Anomalous Light Intensity Dependence of the Rate of Cytochrome c Photooxidation. The kinetics of photooxidation of cytochrome *c* was measured at 550 nm under rectangular shape of excitation of different light intensities with large (oxidized) quinone and (reduced) cytochrome *c* pools at pH 8.4 (Figure 1a). The quinone reduction cycle of the RC was slowed by binding of Ni^{2+} to the main proton entry point of the protein, and its rate of 500 s^{-1} (pH 8.4) decreased by more than 2 orders of magnitude to 3.5 s^{-1} (*25*). At the millisecond time scale, the excitation could be considered as a step function which significantly simplified the evaluation of the response. Because of the linear relationship between the rate constant of the $PQ_A \rightarrow P^+Q_A^-$ charge separation and the light intensity, the intensity of the illumination is measured by the rate constant of the primary photochemistry: 100% light intensity corresponded to a photochemical rate constant of $k_p = 5500$ s^{-1} (at 1 μM RC). At the onset of the continuous illumination, the cytochrome photooxidation showed a fast (1000 s^{-1}) and slightly light intensity dependent initial phase that reflected the generation

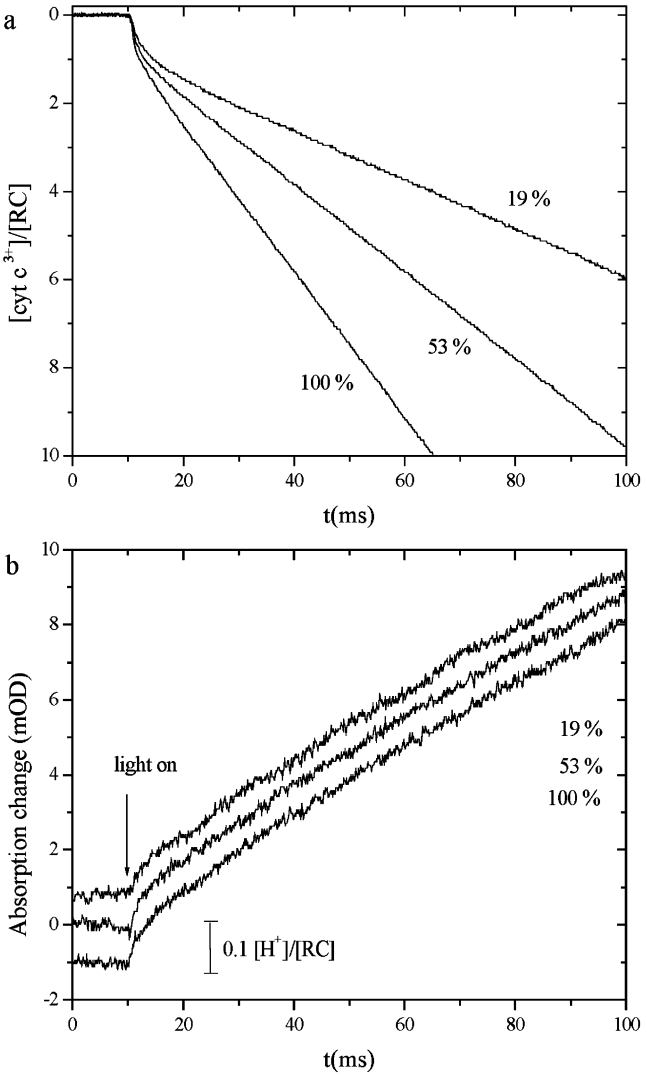

FIGURE 1: Kinetics of cytochrome photooxidation (a) and observed H^+ ion uptake (b) of RC from *Rb. sphaeroides* upon onset of continuous illumination of different intensities. 100% light intensity corresponded to 5 W/cm^2 (808 nm) and 5500 s^{-1} photochemical rate constant. The turnover of the RC was slow due to inhibited proton uptake by binding of Ni^{2+} ions to the protein. The optical absorption changes at 550 nm (a) and 572 nm (b) were converted to concentrations of cyt c^{3+} (a) and H^+ ions (b) relative to that of the RC, respectively. The kinetic traces in (b) were shifted vertically for clear separation. Note the strong light intensity dependence of the rate of the cytochrome turnover (a) in contrast to that of the observed proton binding (b). Conditions: 1 μM RC, 0.03% Triton X-100, 100 μM $NiCl_2$, 40 μM UQ_6, pH 8.4 (both panels), or 60 μM cyt c^{2+} and 60 mM NaCl (a) or 30 μM *o*-cresol red, 150 μM ferrocene, 25 mM NaCl, and ±10 mM Tris (b).

of Q_A^-. The initial phase was followed by an additional transient phase that could hardly be resolved from the stationary phase. Its slope was almost the same as that of the stationary phase, and its magnitude was smaller than one oxidized cytochrome/RC. This transient part of the kinetics could be attributed to the first interquinone electron transfer: its magnitude strongly depended on the equilibrium constant of the electron transfer (*20*) and the rate dropped to 150 s^{-1} as a result of Ni^{2+} binding to the RC (*37*). If the H subunit of the RC was removed, then the magnitude of the transition phases decreased to one oxidized cytochrome/RC that was interpreted by the loss of the Q_B activity of the RC (*10*, *38*). After these transition periods, the constant rate

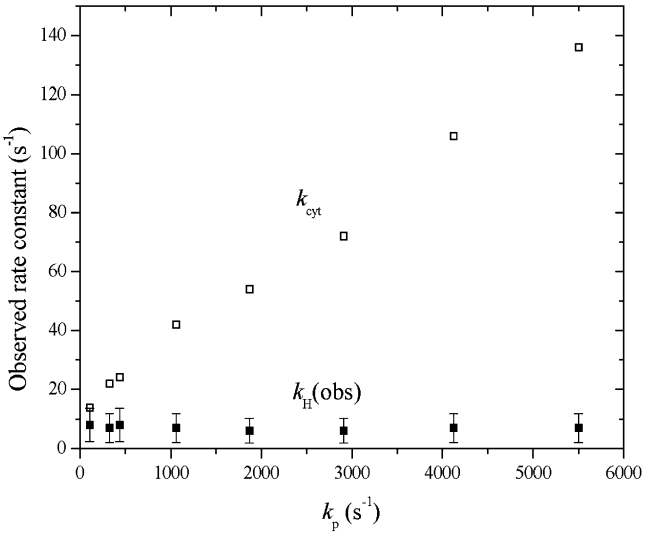

FIGURE 2: Comparison of the light intensity dependence of the rate constants of the turnovers at the donor (□) and acceptor (■) sides of the RC measured by photooxidation of the cytochrome (k_{cyt}) and observed proton binding [k_H(obs)] for quinol formation, respectively. As the RC was treated by 100 μM Ni^{2+}, the proton uptake (k_H) was the rate-limiting step of the photocycle. The intensity of the continuous illumination was expressed by the rate constant of the primary photochemistry (k_p). Note the increasing difference between the two rate constants (acceleration of the cytochrome turnover) upon increasing light intensity. The conditions are the same as in Figure 1a (□) and Figure 1b (■).

of photooxidation of the cytochrome *c* (stationary phase) could be observed that was obviously light intensity dependent (Figure 1a). This was a highly unexpected finding because the light intensity should not be the rate-limiting step in the very slow turnover of the RC. At 100% light intensity, the rate of the primary photochemistry was at least 3 orders of magnitude larger than that of the proton uptake; therefore, the rate of cytochrome turnover should not have been light intensity dependent at all and should have been exactly twice as large as that of the proton uptake. Contrary to this expectation, the rate of cytochrome photooxidation increased linearly from 14 s^{-1} (2%) to 136 s^{-1} (100%) (Figure 2). We set the aim to investigate the origin and consequences of this effect of acceleration.

The inhibition of one of the acceptor side reactions was crucial to observe the acceleration of the cytochrome photooxidation. The effect showed up also if the pH was increased above 9.5 in untreated RC (free of divalent ions) or if one of the key protonatable residues in the proton conduction pathway was mutated to a nonprotonatable form (e.g., AspL213 to Asn). In all of these cases, the rate of the proton uptake dropped and became the rate-limiting step of the turnover. The anomalous increase of the rate of the cytochrome photooxidation was also observed, if the quinone/quinol exchange achieved with low-affinity quinones to the Q_B site (e.g., UQ_0) was the bottleneck of the photocycle (*26*). However, the effect failed if the target of inhibition was the donor side. This was achieved by an increase of the ionic strength of the solution to 150 mM. Under these conditions, the rate of cyt c^{2+} binding to the protein decreased dramatically and became the rate-limiting step of the turnover of the RC (*21*).

The effect of acceleration could be demonstrated in chromatophores, as well. It was shown earlier that the

transition metal ions blocked the proton uptake of RC embedded in the native membrane (*39*). The oxidized dimer was rereduced by the electron donor TMPD (*40*), and the quinone reduction cycle was inhibited by binding of Ni^{2+} to RC. The photooxidation of TMPD was followed at 565 nm. Small increase of the rate was observed upon increase of the light intensity, but the light intensity dependence became more pronounced after addition of UQ_{10} to the chromatophore (data not shown). This indicated the severe loss of quinones in the native membrane due to preparation and also the need of a large quinone pool to generate the effect of acceleration (see also later).

Kinetics of Proton Uptake, Semiquinone Formation, and Superoxide Production. The increase of the rate of cytochrome photooxidation upon increase of the light intensity prompted us to measure the kinetics of chemical species produced by the turnover of the acceptor side. Their kinetic correlation would be of great help to clarify the nature of the observed effect. Unfortunately, the small changes in the absorption spectrum caused by these products are depressed by the large and wide changes due to redox transitions of the cytochrome *c* and other cofactors (P, Q_A) of the RC. This is why we were not able to measure the kinetics of quinol production (in the UV) but were successful in detection of the simultaneous mechanism of proton uptake from the aqueous bulk phase. The loss of H^+ ions from the solution upon continuous illumination of the RC inhibited at the acceptor side showed steady increase (Figure 1b). The rise did not terminate promptly after switch off of the light as the proton uptake to photoproducts was governed by dark reactions (data not shown). In contrast to cytochrome photooxidation, the slope (the rate) of the observed H^+ ion binding did not depend on the light intensity. The decrease of the light intensity from 100% to 20% did not cause measurable change in the rate of the observed proton binding. Despite the relatively large error of the determination of the proton uptake, the difference in rates of proton uptake evoked by continuous and flash lights could be well recognized. The rate of the observed proton binding [k_H(obs)] during continuous illumination was twice as large as that measured after flash excitation (k_H) (Figure 2). Out of the two protons needed for the turnover of the RC inhibited by divalent metal ions, the uptake of the first is slow and that of the second is fast (*1*−*3*, *23*).

The appearance of the effect of acceleration did not depend on what the electron donor to P^+ was. The rate of the photooxidation of ferrocene showed light intensity dependence similar to that of the cytochrome oxidation at an ionic strength where the donation rates of the two donors to P^+ were equal (data not shown). The accumulation of ferricenium during the photocycle could be detected at 300 nm where the contribution of the absorption change due to quinone/quinol conversion is negligible (*41*). If the rate of P^+ rereduction by the electron donor is much larger than that of the rate-limiting proton uptake (this happens if cytochrome is the donor), then the increased rate of the photocycle does not depend on the donation rate.

The magnitude of the enhancement in the rate of cytochrome photooxidation depends on the rate of the slowest step in the photocycle. For demonstration, several methods, including change of the pH and/or use of different divalent transition metal ions, were applied to vary the rate constant

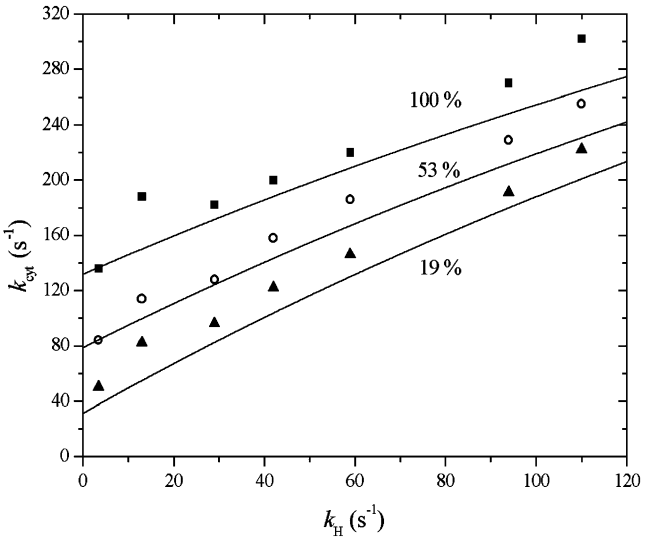

FIGURE 3: Dependence of the rate constant of cytochrome photooxidation (k_{cyt}, acceleration) on the rate constant of the proton uptake (k_H) at different intensities of continuous illumination [100% (k_{p1} = 5500 s^{-1}), 53% (k_{p2} = 2910 s^{-1}) and 19% (k_{p3} = 1040 s^{-1})]. The k_H was varied by changing the pH of the solution and by use of different transition metal ions: Cd^{2+} and Ni^{2+} for adjustment of higher and lower values of k_H, respectively. The k_H remained the rate-limiting step in the photocycle in all cases. Curves to the measured data are derived from the extended photocycle model with parameters of $k_{onq} = 1 \times 10^8$ M^{-1}•s^{-1}, k_{offq1} = 100 s^{-1}, k_{offq2} = 2300 s^{-1}, k_{offs} = 4000 s^{-1}, K_{conf} (=k_+/k_-) = 0.31, and k_c = 1200 s^{-1}. The conditions are the same as in Figure 1a, except for 40 mM NaCl, pH 7−9, and 200 μM $CdCl_2$ (k_H > 20 s^{-1}) or 500 μM $NiCl_2$ (k_H = 3.5 and 13 s^{-1}).

of the proton uptake (k_H) under the same conditions. While the smallest k_H (<20 s^{-1}) values were adjusted by use of Ni^{2+} ion at high pH (>8), faster proton uptake was obtained by use of Cd^{2+} ion at lower pH. The upper limit of k_H was 110 s^{-1} at which value the proton uptake remained the rate-limiting step in the photocycle. As expected, the rate constant of the turnover increased upon increase of k_H and light intensity, and their dependence is close to linearity (Figure 3). However, the relative enhancement of the rate constants upon increase of the light intensity is much larger at small k_H than at high k_H. As the rate constant of the proton uptake determines the amount of the $Q_A^-Q_B^-$ species, we can conclude that the magnitude of the anomalous acceleration of the cytochrome photooxidation depends not only on the light intensity but also on the concentration of the $Q_A^-Q_B^-$ state, as well. Because all of the related data (Figures 2 and 3) show little sign of saturation, linearity in their relationships seems a reasonable assumption under our experimental conditions.

The characteristic absorption change attributed to the semiquinone was measured under continuous illumination in the presence of cytochrome at 337 nm (isosbestic wavelength for the cyt c^{2+}/c^{3+} and quinone/quinol redox change) and at 450 nm (absorption peak of the anionic semiquinone) when ferrocene was the electron donor to P^+. The isosbestic wavelength at 337 nm was adjusted by intact RC (without Ni^{2+} ion) where no accumulation of $Q_A^-Q_B^-$ species but that of cyt c^{3+} and quinol were expected. If divalent metal ion was added to the sample, a large absorption change was measured immediately after onset of the excitation due to the appearance of stable $Q_A^-Q_B^-$ species in the RC. However, no further significant change in the

stationary phase of the turnover was detected, indicating the absence of accumulation of semiquinone produced by dissociation. The same result was obtained in experiments with ferrocene at 450 nm (data not shown).

The accelerated turnover was accompanied by production of a substantial amount of superoxide anion. Upon addition of NBT, the kinetics of accumulation of a new photoproduct could be clearly observed at one of the isosbestic points of the cytochrome redox change (541 nm, Figure 4a). Taking the difference of the light-induced absorption changes between 450 and 700 nm in the presence and absence of NBT, the spectrum of reduced NBT (diformazan) with a maximum at 530 nm was identified. The reduced NBT was stable for minutes as could be clearly seen by overlap of the steady-state spectrum recorded after illumination with the spectrum constructed from kinetic data (Figure 4b). The superoxide radical can react also with the oxidized cytochrome produced by the photocycle. This reaction will be more effective if a significant amount of chemically oxidized cytochrome is available and can be visualized by a slightly smaller steady-state rate of cytochrome turnover and slow reduction of cyt c^{3+} in the dark (Figure 4c). The production of superoxide anion was confirmed by addition of SOD that inhibited the reduction of cyt c^{3+} by facilitation of the dismutation of the superoxide radicals. The steady-state rate of production and dark decay of cyt c^{3+} were only slightly influenced by denatured SOD (Figure 4c).

Availability of Quinones and Herbicides to the Q_B Binding Site. The rate of cytochrome photooxidation in the RC with retarded proton uptake depends not only on the light intensity and k_H but also on the external quinone concentration, as well. While at small quinone concentration, the acceleration could hardly be observed, the large quinone pool size favored the appearance of the effect. The titration of quinone at constant light intensity showed saturation in wild-type RC treated by Ni^{2+} ions (Figure 5a). Similar saturation was observed in mutant RC (L212Glu → Gln/L213Asp → Asn) where the uptake of the proton was similarly severely hindered but the rate of the first interquinone electron transfer was not significantly decreased compared to that in the wild-type RC (data not shown). The quinone concentration at half of the saturation rate was much larger than the equimolar (UQ/RC = 1) concentration and increased slightly upon light intensity. The turnover rate measured at different quinone levels showed a steep rise as a function of light intensity, and the slope increased with quinone concentration (Figure 5b). No tendency for saturation can be seen in these ranges of light intensity whatever quinone concentration is taken. The experiments carried out with different types and concentrations of detergents showed that the quinone availability to the Q_B binding site (and not its concentration) was essential to produce the effect of acceleration.

The results of these experiments support the assumption of modification of the Q_B binding site. Because the quinone undergoes redox change after binding, the alterations in its binding properties can hardly be utilized directly to monitor the structural change in the protein. Instead, potent electron transfer inhibitors stigmatellin and terbutryn were used to test the possible modification of the binding site. The binding affinity of the antibiotic stigmatellin was studied in competition with strongly binding UQ_6 to the Q_B site under continuous excitation (Figure 6). The concentration of UQ_6

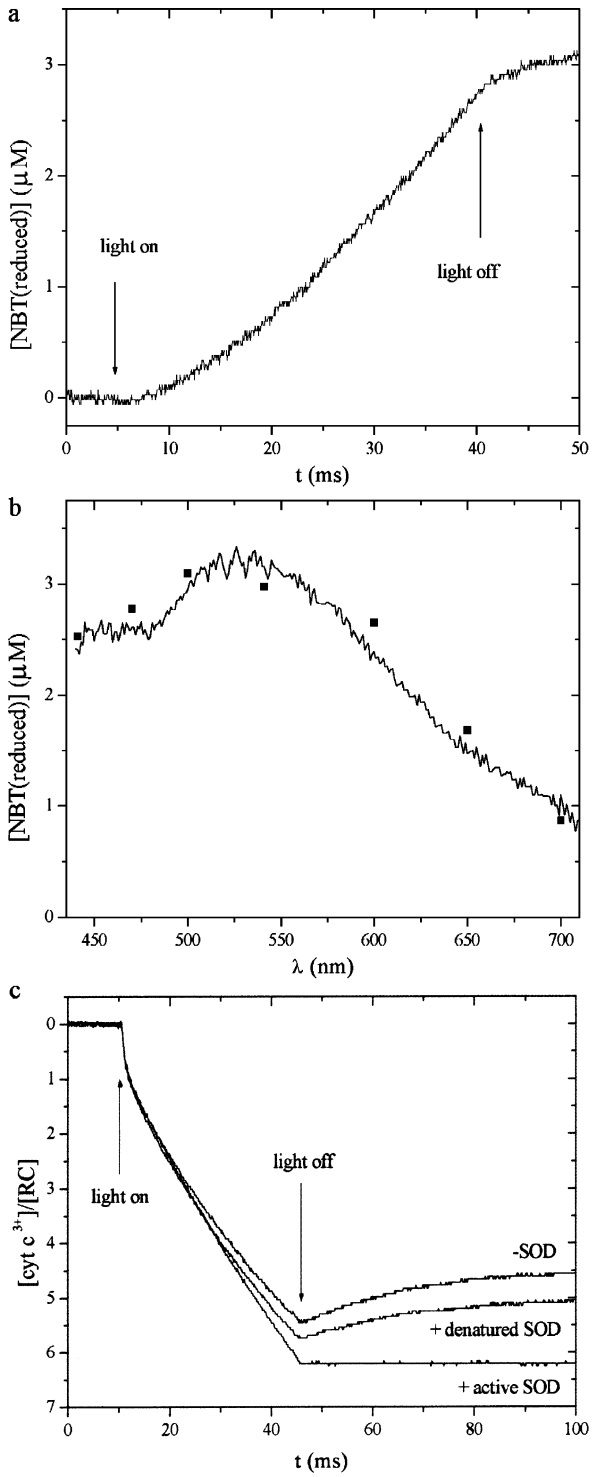

FIGURE 4: Production of superoxide radical during the photocycle of RC of inhibited proton uptake. The NBT assay for superoxide synthesis was applied to determine the number of escaped electrons from the standard photocycle of the RC. (a) Kinetic trace at the isosbestic wavelength of the cytochrome (541 nm) solely due to production of reduced NBT. (b) The difference of absorption changes measured in the presence and absence of NBT at the termination (35 ms) of the excitation (■) and long (about 1 min) after the illumination (line). The oxidized NBT had no absorbance in this spectral range. (c) Cytochrome assay for superoxide synthesis. By setting a large cyt c^{3+} pool, effective dark reaction due to the reduction of cyt c^{3+} by superoxide radical can be observed. The reaction is inhibited by addition of active SOD. Denatured SOD had a minor effect. The conditions are the same as in Figure 1a, except for ±10 μM NBT (a and b) and [cyt c^{2+}] = [cyt c^{3+}] = 33 μM and ±20 units/mg SOD (c).

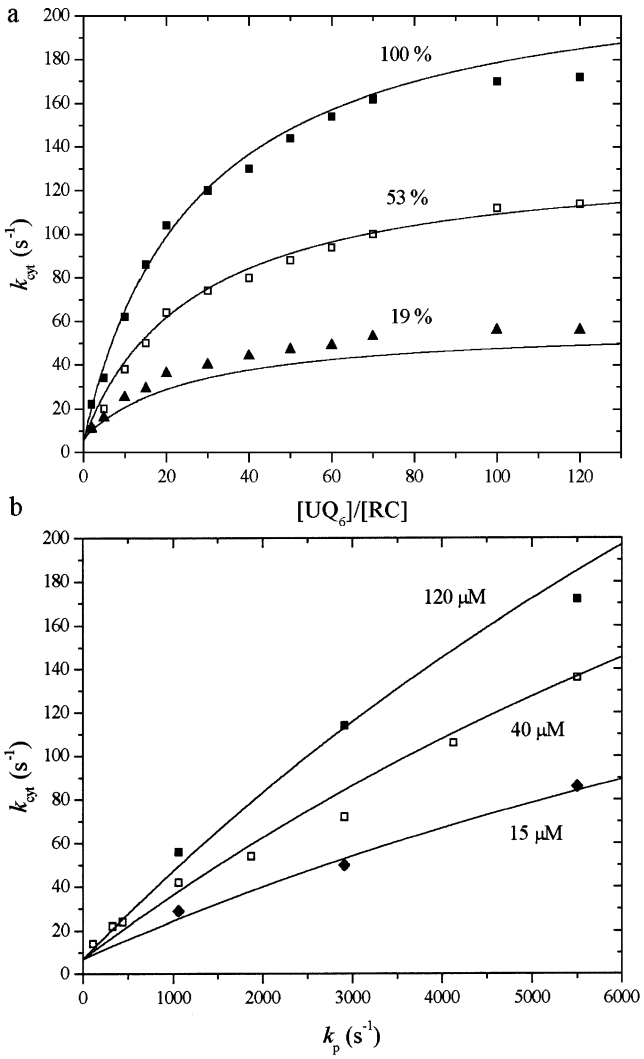

FIGURE 5: Dependence of the rate constant of cytochrome photooxidation (k_{cyt}) on the concentration of added quinone at different intensities of continuous excitation (100%, 53%, and 19%) (a) and on the light intensity at different levels of UQ_6 (15, 40, and 120 μM) (b) in RC of inhibited proton uptake. The simulated curves from the model were obtained by use of parameters in Figure 3 and $k_H = 3.5\ s^{-1}$. The conditions are the same as in Figure 1a, except for 500 μM Ni^{2+} and 40 mM NaCl.

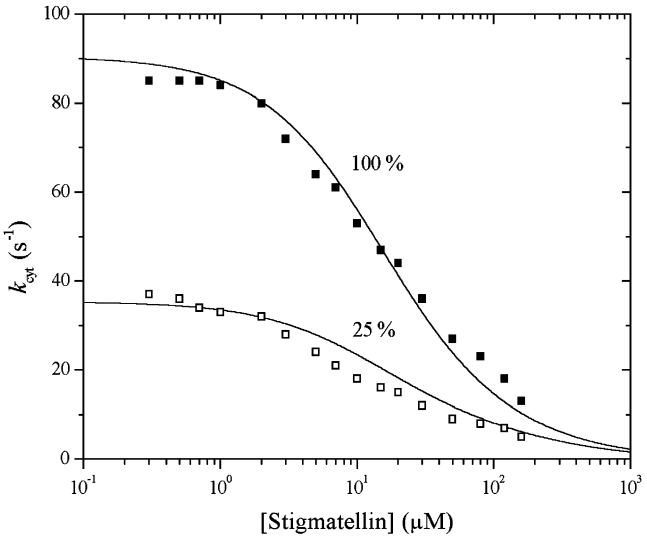

FIGURE 6: Deceleration of the stationary rate of cytochrome photooxidation (k_{cyt}) upon titration of stigmatellin in the presence of UQ_6 in RC of slow proton uptake at different intensities of continuous light excitation [100% ($k_{p1} = 5500\ s^{-1}$) and 25% ($k_{p2} = 1375\ s^{-1}$)]. The curves are derived from the model with parameters as in Figure 5 and $k_{oni} = 6.6 \times 10^4\ M^{-1}\cdot s^{-1}$, $k_{offi1} = 0.033\ s^{-1}$, and $k_{offi2} = 0.6\ s^{-1}$. The conditions are the same as in Figure 1a, except for 15 μM UQ_6.

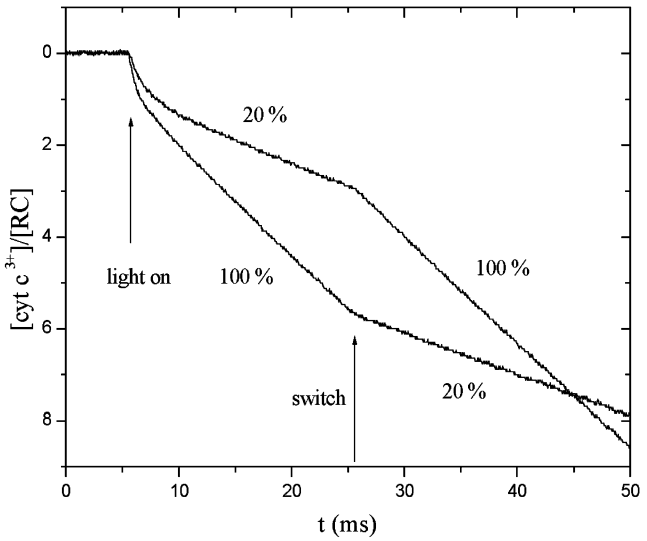

FIGURE 7: Changes of the rate of cytochrome photooxidation [k_{cyt}(low) = 96 s^{-1} and k_{cyt}(high) = 220 s^{-1}] upon switch from low (20%) to high (100%) (top) and from high to low (bottom) light intensities in RC of inhibited acceptor side turnover. The switch of the light intensity was fast (<1 μs), and the response of cytochrome turnover cannot be resolved in this time scale. The conditions are the same as in Figure 1a except for 200 μM $CdCl_2$.

was taken as 15 μM, which was an optimum selection between not too strong competition with stigmatellin and not too short steady-state period of the turnover of the RC. Upon increase of the concentration of the stigmatellin, the rate of cytochrome photooxidation was titrated with characteristic effective inhibition constants (I_{50}, at the equivalent concentration, where the rate of cytochrome photooxidation drops to half of the maximum value). The I_{50} of the stigmatellin showed changes at different light intensities. Stronger illumination made the stigmatellin less effective: 4 times more intense excitation (from 25% to 100%) doubled the effective inhibition constant. Similar loss of effectiveness due to high light excitation of the RC with inhibited acceptor side turnover was measured for terbutryn (data not shown). The shift of the I_{50} of terbutryn was so large that its determination was limited by the solubility of the terbutryn in the aqueous sample. A similar decrease of the affinity of the terbutryn to the Q_B site as we observed at high light intensity was reported in the LM complex where the inhibition constant increased by 2 orders of magnitude to 300 μM after removal of the H subunit (*10*).

Switch between Low and High Light Intensities. To get an impression of how fast the response of the photocycle could be to sudden changes in the light intensity, the output power of the laser diode was increased or decreased promptly (transition time <1 μs) during the steady-state regime of the photocycle (Figure 7). In the millisecond time range, we were not able to observe any transition phases after the switch. The photocycle accommodated to the new light conditions (independently of the direction of the change in the light intensity) without measurable delay and switched im-

mediately to the altered (new) rate. No transients were detected on the whole temperature range of physiological significance (data not shown). Although the determination of the rate of conformational switch was not possible, a lower limit can definitely be given: the rates of (yet unknown) processes involved in the (conformational) change of the protein should be 10^3 s^{-1} at least.

DISCUSSION

We observed a light intensity dependent rate of cytochrome photooxidation where the turnover of the acceptor side in RC was inhibited. A series of simple experimental strategies were applied to study this system whose utility seems clear to establish new and interesting properties of the protein.

Origin of the Acceleration. The enhancement of the rate of cytochrome photooxidation in RCs treated by Ni^{2+} ion is not related to donor side processes but corresponded clearly to the modification of the "normal" function of the acceptor quinone complex. Due to the inhibited H^+ ion uptake, the RC is trapped in the $Q_A^-Q_B^-$ state for a long period of time (100 ms), and new photooxidized cyt *c* should appear only after proton delivery to Q_B^-. However, we observed extra cyt c^{3+} production that was not correlated to proton uptake. To identify its origin, several possibilities were considered.

(a) Double Reduction of Q_A or Q_B and Release from RC before Protonation. This is certainly an alternative way of additional cyt c^{3+} production (i.e., acceleration) whose reality can be supported partly by some earlier experimental results. Double reduction of Q_A was observed after chemical prereduction of Q_A by sodium dithionite to Q_A^- upon continuous high light excitation (*42*). As the production of Q_A^{2-} occurred in the time scale of seconds, its possible release should be very slow to assume to be operative in our case.

The wealth of experimental information about the chemical reduction of the cofactors by $NaBH_4$ can also be utilized (*10*, *43*, *44*). $NaBH_4$ reduces Q_B to the Q_B^{2-} form without reacting with Q_A. (Sodium borohydride is a two-electron reductant.) The equilibrium established between the $Q_AQ_B^{2-}$ and $Q_A^-Q_B^-$ states is pH dependent and favors the formation of the $Q_A^-Q_B^-$ state above pH 8.5. The result can be applied to disproportionation of the two light-induced electrons in the acceptor quinone system. The formation of the $Q_A^-Q_B^{2-}$ state under continuous excitation likely decreases the binding affinity of Q_B^{2-}; therefore, it dissociates from the binding site, and the generation of a new $Q_A^-Q_B^-$ state would enhance the rate of cytochrome turnover. However, this mechanism as the main contributor to the acceleration can be disregarded for two reasons: (1) The dissociated Q_B^{2-} has a very high pK_a [>12 (*12*)]; thus it would be immediately protonated in solution and would cause an increased rate of proton uptake. However, this was not observed in our experiments. (2) The semiquinone biradicals ($Q_A^-Q_B^-$) induced by flashes have been proven very stable in the dark and did not show remarkable disappearance in the time range used in our study. Therefore, the conversion of semiquinone biradicals to Q_B^{2-} is negligible under our conditions.

(b) Unstable Q_B^- Semiquinone Anion. It has long been accepted that the anionic (not protonated) semiquinone is tightly bound to the protein (*13*) and its properties (stability) are defined by the environment of the Q_B site (*45*). If the H subunit of the RC protein was removed, the lifetime of Q_B^- decreased by a factor of 10^3 (from 250 to 0.3 s at pH 7.7 and 21 °C), and the electron leaking off Q_B^- was taken up by the oxidized cytochrome *c* (*10*). If the RC is embedded in an alkane-containing phospholipid membrane, the binding affinity of the semiquinone anion formed in the Q_B site is orders of magnitude weaker than in the native system. The semiquinone can be exchanged for quinone from the membrane−quinone pool, move away from the site, and accumulate in the membrane. Certain water-soluble benzoquinones reduced to semiquinone in binding sites of the RC in aqueous media tend to diffuse away into the solution (*46*).

In the instability of Q_B^-, the oxygen can play a significant role which has been only partly revealed. Although the quinol is generally unreactive with molecular oxygen, the semiquinone form, either in the Q_B site or free in the membrane, is much more reactive (*46*). During the interaction of oxygen with Q_B^-, reduced oxygen species, such as the superoxide anion radical, can be generated as was revealed in aerobic samples under continuous illumination (*47*). The efficiency of the interaction was determined by the conformational transitions in the structure of the RC triggered by the actinic light.

In the crystal structures, two (proximal and distal) binding sites for Q_B were identified (*9*, *48*). Although no direct evidence for quinone reduction in the distal site was found, pH-temperature- and structure-dependent disproportionation in the location of the quinone between the two binding sites was assumed (*49*, *50*), and the redox- and dissociation free energies of the semiquinone at the distal position were calculated (*12*). Calvo et al. trapped the semiquinone biradical in the photosynthetic RC and measured the EPR spectra at temperatures between 1.5 and 100 K (*44*). The relative position and orientation of the two quinones in the biradical state ($Q_A^-Q_B^-$), determined from the EPR spectra, compared well with those obtained from X-ray diffraction of the RCs in the $Q_AQ_B^-$ state (*9*). The Q_A did not rotate upon reduction to Q_A^-, and the Q_B^- did not move relative to Q_A^- (the distance between the centers of the quinone rings remained constant). The only difference between the two structures involved a relative rotation of the quinone planes that made these planes nearly parallel in the biradical state. This indicated a change in the orientation of Q_B^- produced by the electrostatic interaction between Q_A^- and Q_B^-. Although the conditions and properties were different in these examples, clear parallels of loss of structural and functional stability of Q_B^- can be recognized in these systems.

The protonation of Q_B^- either released or displaced in the RC should not be favored since no acceleration of proton binding is observed in our experiments. Indeed, the pK_a of the semiquinone form of UQ_{10} is low: 6.45 in methanol (*51*) and 5.9 in 7 M 2-propanol/1 M acetone (*52*). In aqueous phase, pK_a = 4.9 can be deduced from the known solvent effect on the pK_a of durosemiquinone (DQ^-) (*2*, *12*). The relevant pK_a for Q_B^- in the $Q_A^-Q_B^-$ state, where the influence of the Q_A^- anion is significant, is somewhat (by 0.7 unit) higher as revealed from results with rhodoquinone acting as Q_B (*53*). Hence, it is reasonable to consider that the unstable semiquinone anion is not protonated under our conditions (pH >6).

What will happen to the dissociated anionic semiquinone? As no accumulation was observed during the photocycle, the rate of oxidation of the dissociated semiquinone had to be high. Indeed, Swallow measured the rate constants for electron transfer reactions of semiquinones in aqueous solutions and found their values to be as high as about 5×10^9 $M^{-1}\cdot s^{-1}$, close to the diffusion-controlled limit (*54*). Detection of the superoxide anion showed that in our experiments the oxidation of Q^- by oxygen was the major route of escape of the electrons: $Q^- + O_2 \leftrightarrow Q + O_2^-$, where O_2^- represents an oxygen molecule with an extra (unpaired) electron. The reaction is (in standard terms) energetically unfavorable as the midpoint redox potentials of Q/Q^- and O_2/O_2^- are -145 mV (see later) and -330 mV (*55*), respectively. Despite the uphill transfer, the equilibrium is shifted to the direction of generation of O_2^- during illumination. Since the NBT is a two-electron oxidant, the produced ~2.7 [NBT]/[RC] (Figure 4a) at the end of the illumination accounts for the number of escaped electrons calculated as the difference of electrons injected from oxidation of cytochrome [~6.2 [cyt^{3+}]/[RC] (Figure 4c)] and exported electrons via generation of quinol [0.25 [H^+]/[RC] (=0.125 [QH_2]/[RC]) calculated to the same time regime using $k_H(obs) = 7\ s^{-1}$]. After removal of oxygen from the solution, other routes of semiquinone oxidation will play a dominant role: (1) oxidation by the secondary donor system (cyt c^{3+}) that is believed to be slow (*56*) and (2) dismutation with another Q^- to give Q and QH_2. This, too, will be slow as the rate constant will depend on the concentration of escaped Q^-.

(c) Possible Driving Force of the Conformational Changes. In agreement with earlier literature data, the stable semiquinone biradical $Q_A^-Q_B^-$ produced by two flashes and trapped by inhibited proton uptake was observed at room temperature. However, if this intermediate state is produced during continuous excitation, the redox, energetic, and conformational conditions could be significantly different. The $Q_A^-Q_B^-$ state is considered to be "closed" for productive photochemistry, because P^+Bpheo^- recombines so quickly (<10 ns) that no trapping can occur by either electron transfer to P^+ or from $Bpheo^-$ in less than 1 s. The P^+Bpheo^- charge pair is produced with relatively high frequency (10^4 s^{-1}) at the largest light intensity used in our experiments. Trapping of $Bpheo^-$ by reduction of P^+ by cytochrome c^{2+} was detected at a time scale of seconds after chemical reduction of Q_A. Contrary to the effect in our case, the efficiency of trapping showed strong dependence on the donation rate by cytochrome c^{2+} (*42*). The electrostatic interaction energy between Q_B^- and Q_A^- is moderately high [1.1 $\Delta pK = 2.56$ k_BT (*57*)]. Because the distance between the centers of the Q_B and Q_A rings (18.6 Å) is comparable to that of Q_B and Bpheo (24.4 Å) (*9*), the electrostatic interaction energy will increase substantially by increase of the light intensity. The magnitude of the repulsive electrostatic interaction between Q_B^- and $Bpheo^-Q_A^-$ (activation "barrier") and the frequency of appearance of $Bpheo^-$ ("collision" frequency) can ensure a measurable reaction rate of activation (transition state) process leading to a product state characterized by shift of the equilibrium position and/or of larger rotation of the plane of Q_B^-. The phenomenon is similar to the physiological law of sensation known as summation of stimuli under threshold. This qualitative picture should be supported by an adequate transition state theory of conformational changes including exact electrostatic and quantum chemical calculations.

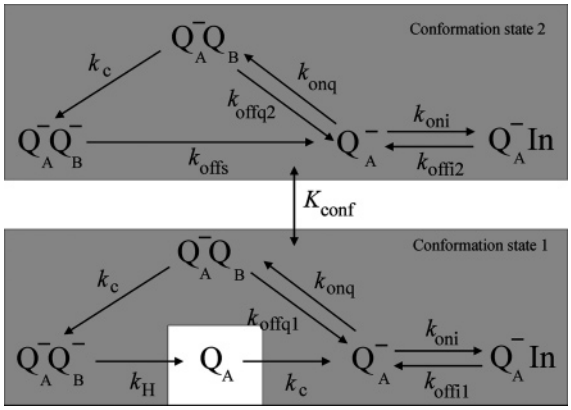

FIGURE 8: Extended kinetic model of the photocycle to explain the uncoupling of the electron and proton transfers in RC of inhibited acceptor turnover. Short-lived states and fast reactions are omitted. The RC can be found in two conformation states (1 and 2). The equilibrium constant between the states (shaded) involved in conformation change is denoted by K_{conf}. In conformation state 1, a conventional photocycle is taking place. The rate-limiting reaction is the proton uptake (k_H) that enables the accumulation of the $Q_A^-Q_B^-$ state and favors the light-induced conformational transition. In conformation state 2, Q_B^- dissociates readily from the RC (k_{offs}). In both conformations, quinone (k_{onq}) or inhibitor stigmatellin (k_{oni}) from the pool(s) can bind to the empty binding site in the Q_B pocket. The photocycle in conformation state 2 will not produce quinol and thus increases the uncoupling of electron and proton transfer through the protein. For notations, see the abbreviations.

Model of the Extended Photocycle. Our observation of acceleration of the cytochrome photooxidation in the RC of inhibited quinone turnover cannot be explained by a conventional model of the quinone reduction cycle (*58*) but calls for modifications due to altered kinetic and thermodynamic properties of the semiquinone and quinone under high light conditions (Figure 8).

The essential alteration includes a light-induced change of the Q_B binding pocket in the protein resulting in a much more favored exchange of Q_B^- for a quinone from the pool. Presently, the exact nature of the modification cannot be predicted. It may include a shift of Q_B^- from the proximal to distal position or a suited change of the protein environment around the catalytic binding site. In both cases, the immediate environment of Q_B is changed, which will be expressed here by *conformational transition* (CT) defined by the concentration of the RC in the modified (denoted by subscript 2) conformation referred to the total concentration:

$$CT = [RC]_2/[RC] \quad (1)$$

The forward rate of the conformational change is proportional to the light intensity and the concentration of the RC (precursor) species capable of conformational transition: $k_+ I [Q_A^-(...)]_1$. Here $Q_A^-(...)$ means the photochemically trapped RC (independently what is in the Q_B site), and subscript 1 refers to the unmodified conformation state of the RC. The backward rate is proportional to the concentration of the RC in the modified (2) conformation: $k_-[RC]_2$. In equilibrium, the two rates are equal:

$$K_{conf}\, I\, [Q_A^-(...)]_1 = [RC]_2 \quad (2)$$

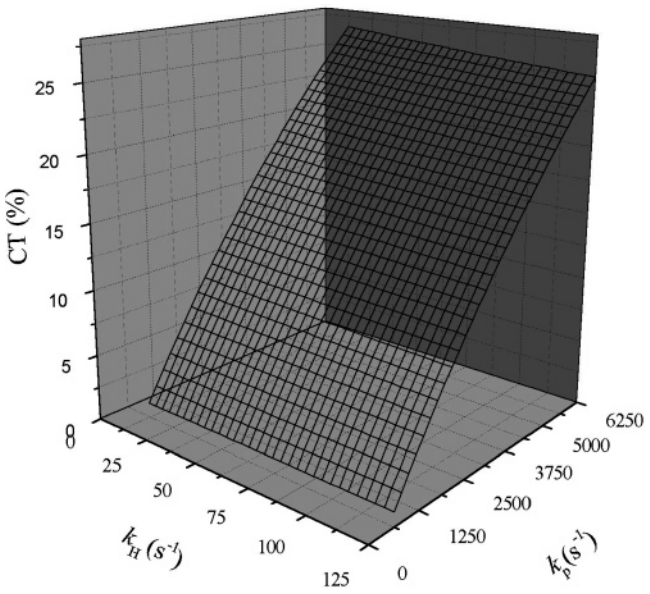

FIGURE 9: Pseudo-3D map of the dependence of the conformational transition (CT) on the light intensity (expressed in terms of k_p) and on the rate constant of the (first) proton uptake, k_H. CT was derived from eq 1, and the stationary concentrations of the intermediates in conformation 2 were calculated from the extended photocycle model using 1 μM RC and 40 μM UQ_6 (Figure 8).

where $K_{conf} = k_+/k_-$ is the equilibrium constant of the conformational change.

The reactions of the photocycle in the two conformation states of the RC are somewhat different. For the sake of simplicity, only the important and slow reactions will be considered, which determine the rate of the turnover (Figure 8). The photocycle in conformation state 1 consists of well-known steps including the two light reactions together with the photooxidation of the cytochromes (effective rate constant k_c), the quinone binding/unbinding reactions (rate constants k_{onq} and k_{offq1}, respectively), and the proton uptake (rate constant k_H). The photocycle is simplified in the (modified) conformation state 2 due to the decreased affinities of the semiquinone and the quinone to the binding site. The semiquinone dissociates from the RC (rate constant k_{offs}), and the unbinding rate constant of the quinone (k_{offq2}) is also modified. No proton uptake, no quinol production, and oxidation of only one cytochrome are associated to this set of reactions. The observed rate of the photocycle of the RC is the weighted sum of those of the two processes (for quantitative details of the model, see Supporting Information). By introduction of the modified conformation state, more photooxidized cytochromes will be generated without increase of the quinol production. Formally, the electron transfer and the proton uptake become uncoupled: the electron transfer through the protein runs faster than the proton uptake, and the stoichiometric ratio of transferred electrons to bound protons (e/H^+) increases. The dissociation of Q_B^- from the protein in its modified conformation state wastes the absorbed photon's energy and lowers the yield of photoconversion in the RC.

The comparison of the set of measured data with predictions of the model should answer two basic questions: what fraction of the RC enters the altered conformation state and what are here the dissociation properties of the semiquinone and quinone. The model contains formally three adjustable (fitting) parameters: K_{conf}, the equilibrium constant of the conformational change, and k_{offq2} and k_{offs}, the unbinding rate constants of the quinone and semiquinone in the modified conformation state of the RC, respectively. The values of the other rate constants or dissociation constants can be taken from previous work [$k_{onq} = 1 \times 10^8$ $M^{-1}\cdot s^{-1}$ and $k_{offq1} = 100$ s^{-1} (*59*, *60*)] or measured directly (k_p, k_c, and k_H). Consult the figure legends for their actual values. By solution of the equations derived from the model under steady-state condition together with eq 2, the measured data of the quinone titration (Figure 5a) and the dependences of the light intensity (Figure 5b) and the rate of proton uptake (Figure 3) could be well simulated using the same set of parameters in all cases. From eq 1, the values of the conformational transition can also be calculated as a function of two important experimental variables, the light intensity and the rate constant of the proton uptake (Figure 9). k_p and k_H have opposite effects with different magnitudes and slopes on the conformational transition. In our experiments, not much deviation from the linearity is observed up to the highest light intensity and lowest proton uptake where the CT rises as high as 25% if the concentrations of the RC and UQ_6 are 1 and 40 μM, respectively.

The stoichiometric ratio of the transferred electrons to bound protons (e/H^+) can be directly derived from the model. The expression reduces to

$$\frac{e}{H^+} = 1 + \frac{K_{conf}\, I}{1 + K_{conf}\, I}\left(\frac{k_{cycle2}}{2\, k_{cycle1}}\right) \qquad (3)$$

if $k_p > 500$ s^{-1} and $k_H < 50$ s^{-1}. Here k_{cycle1} and k_{cycle2} are the rates of the photocycle in conformation states 1 and 2, respectively, and $K_{conf} = 0.31$ if I is measured relative to its highest value. As the reactions in both photocycles are coupled in series, the reciprocal value of the overall rate, $(k_{cycle})^{-1}$, is the sum of the reciprocal values of the rates of the individual steps. Each turnover delivers two electrons and two protons in conformation 1 and only one electron in conformation 2. The uncoupling of the electron transfer and the proton binding is a linear measure of the ratio of the cycling rates in the two conformations of the RC, and its light intensity dependence is close to linearity in this range. At the highest light intensity and the slowest proton uptake used in our experiments, $k_{cycle1} = k_H = 3.5$ s^{-1} and $k_{cycle2} = 550$ s^{-1} ([Q] = 40 μM); thus the stoichiometric ratio of uncoupling can be as high as $e^-/H^+ = 20$.

The rate constant of the semiquinone dissociation from the protein in the modified binding position (environment) is high ($k_{offs} = 4000$ s^{-1}), and its dissociation constant (40 μM) resembles that of the quinone to the same binding site (23 μM). This opens the way for comparison with similar experiments in the Q_A binding site. Identical dissociation constants were observed for the neutral duroquinone and the negatively charged 5-OH-NQ at the Q_A site, but the on/off rates of the former were 4 orders of magnitude larger than those of the latter (*61*). The authors argued for a kinetic trap of 5-OH-NQ due to the negative charge on the quinone. In the modified Q_B binding site, the (neutral) quinone and the anionic semiquinone have comparable affinities independently of their charges. In contrast to the Q_A site, the negative charge on the semiquinone does not induce response of the (modified) Q_B site to favor the kinetic trap. Our experiments

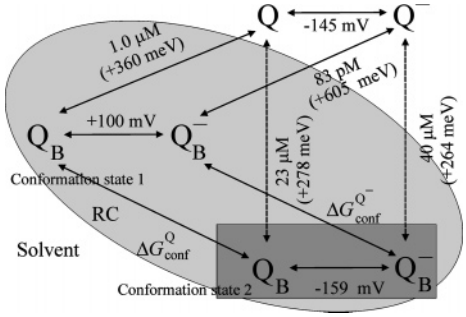

FIGURE 10: Thermodynamic model including the redox changes of the quinones in three locations (in aqueous solvent and in two conformations of the Q_B pocket of the RC), their dissociation from the protein, and the conformational changes of the Q_B binding sites. The numerical values were taken from experiments (refs *18*, *59*, *60*, *65*, and *66* and the present study), estimated on the basis of the electrochemistry of semiquinones (*54*), or determined from the corresponding thermodynamic boxes.

indicate that the charge-induced interactions responsible for modification of the protein environment are very sensitive to the location.

The model can be applied to determine the increased dissociation constant of the stigmatellin at high light intensity (Figure 6). In both conformation states of the RC, the stigmatellin competes for the Q_B binding site with the quinone. As a result of this competition, the dissociation constant of $k_{offi1}/k_{oni} = 0.5$ μM was determined from charge recombination measurements at pH 8.5 (*62*), which refers to the RC with no light-induced conformational changes in the Q_B pocket. The values of $k_{offi1} = 0.033$ s^{-1} [pH 7.2, *Rhodobacter capsulatus* chromatophore (*63*)] and $K_D = 0.5$ μM increased at the highest light intensity ($k_p = 5500$ s^{-1}) 18 times to $k_{offi2} = 0.6$ s^{-1} and $k_{offi2}/k_{oni} = 9.1$ μM, respectively. The large shift of the dissociation constants in the two conformations is reflected moderately in the apparent inhibition constants (e.g., I_{50} values) shown in Figure 6, because the two light intensities (100% and 25%) at which proper titrations could be carried out offered closely related combinations of the two conformations (see Supporting Information). The less effective binding of the stigmatellin comes from the increased off rate (from 0.033 to 0.6 s^{-1}) in the modified binding site, similarly to the semiquinone and the quinone response to the conformational change. This is a strong support for structural changes in the Q_B binding pocket caused by high light excitation. The conformational change seems to be relatively independent of the cofactors of the protein, which are only sensors but not producers of the changes in the protein conformations. Similar conclusions were drawn from FTIR difference spectroscopy measurements at the Q_A site (*64*). The appearance of the semiquinone caused structural changes, which did not depend on the substituents on the quinone ring.

Difference of Free Energies of Q and Q⁻ for Conformational Changes. Three independent thermodynamic boxes can be constructed in the scheme involving dissociation from the RC and one-electron redox changes of the quinone in three different locations: in aqueous solution and in the binding sites of the Q_B pocket corresponding to the two conformation states of the RC (Figure 10). Although the rate of oxidation of semiquinone in aqueous solution is high, it will be supposed not to perturb the binding equilibrium of semiquinone in the Q_B site. The free energy changes associated with the reduction of the quinone, $\Delta G^{Q/Q^-} = -F(E_h - E_m)$, can be related to the free energy changes of the dissociation, $\Delta G_D = -60$ meV logK_D (at room temperature), and conformation, ΔG_{conf}:

$$\Delta G_{D1}^{Q_B} + E_{m1,Q_B} - \Delta G_{D1}^{Q_B^-} - E_{m,sol} = 0 \quad (4)$$

$$\Delta G_{D2}^{Q_B} + E_{m2,Q_B} - \Delta G_{D2}^{Q_B^-} - E_{m,sol} = 0 \quad (5)$$

$$\Delta G_{conf}^{Q} + E_{m2,Q_B} - \Delta G_{conf}^{Q^-} - E_{m1,Q_B} = 0 \quad (6)$$

Here F is the Faraday constant (used to convert units of electric potential to units of energy and vice versa), E_h is the actual redox potential, E_m is the midpoint redox potential at pH 7, K_D is the dissociation constant, and subscripts 1 and 2 refer to the two conformation states of the Q_B binding pocket. Their numerical values related to the transitions were either taken from the experiments directly [$E_{m1,Q_B} = +100$ mV (*65*), $K_D^Q = 1.0$ μM (*60*)] or calculated from $E_{m,Q_B} = E_{m,Q_A} + 60$ mV log K_2, where $E_{m,Q_A} = +30$ mV at pH 7 (*18*) or +10 mV at pH 7 (*66*) and the one-electron equilibrium constant was $K_2 = 13$ (pH 7). The determination of the other parameters was based on reasonable estimates [$E_{m,sol} = -145$ mV (*12*) and $k_{on} = 1 \times 10^8$ $M^{-1}\cdot s^{-1}$ for both quinone and semiquinone] or was calculated from the relevant thermodynamic box. The $E_{m,sol}$ for ubiquinone in aqueous solution is disputed: larger [−100 to −120 mV (*67*)] and smaller [−230 mV (*54*) and −350 mV (*68*)] values are also used in different analysis of quinone electrochemistry. The dissociation constants of the semiquinone and the quinone increased (the binding affinities decreased) upon conformational change of the binding pocket by 4.8×10^5 and 23, respectively. This change in protein conformation required 259 meV more free energy if the Q_B binding site was occupied by semiquinone instead of quinone: $\Delta G_{conf}^{Q^-} = \Delta G_{conf}^{Q} + 259$ meV. That amount of free energy (5.9 kcal/mol) may cover the energy cost to break H-bond(s) of the semiquinone to L190His and/or L212Glu.

The redox midpoint potential of −159 mV was deduced for the Q_B/Q_B^- redox pair at the modified binding position. This value is very close to that estimated in aqueous solution (−145 mV). This means that the positive electrostatic potential (provided by charges, protein backbone dipoles, or H-bond donors) which usually increases the E_m of the quinone bound to the protein does not have significant effect in conformation state 2 of the RC; i.e., the quinone at the modified Q_B binding position feels as in aqueous solution. On the other hand, the midpoint potential of −159 mV is 100 mV more positive than that calculated for the distal binding position [−260 mV, using $E_{m,sol} = -145$ mV (*12*)]. Consequently, we can argue for a conformational change of the RC rather than for a shift of the Q_B binding position in the RC of the unaltered structure.

The functional analysis carried out in this work should be supported and extended by structure-oriented investigations in the future to understand the nature of the conformational change including the location of the (semi)quinone (or inhibitors) in the Q_B binding pocket under accelerated cycling of the RC.

ACKNOWLEDGMENT

We are indebted to Dr. G. Laczkó (University of Szeged) for construction of the switching mode of the laser diode and to Dr. E. Hideg (Biological Research Center, Szeged) for generous support in identification of reactive oxygen species.

SUPPORTING INFORMATION AVAILABLE

The model of conformational equilibria with competitive quinone, semiquinone, and inhibitor binding to the Q_B site is explicitly formulated and the equations are solved. This material is available free of charge via the Internet at http://pubs.acs.org.

REFERENCES

1. Paddock, M. L., Feher G., and Okamura, M. Y. (2003) Proton-transfer pathways and mechanism in bacterial reaction centers, *FEBS Lett. 555*, 45−50.
2. Wraight, C. A. (2004) Proton and electron transfer in the acceptor quinone complex of photosynthetic reaction centers from *Rhodobacter sphaeroides*, *Front. Biosci. 9*, 309−337.
3. Wraight, C. A. (2005) Intraprotein proton transfer-Concepts and realities from the bacterial photosynthetic reaction center, in *Biophysical and Structural Aspects of Bioenergetics* (Wikström, M., Ed.) pp 273−312, RSC Biomolecular Science Series, Royal Society of Chemistry, Cambridge, U.K.
4. Namslauer, A., Pawate, A. S., Gennis, R. B., and Brzezinski, P. (2003) Redox-coupled proton translocation in biological systems: Proton shuttling in cytochrome *c* oxidase, *Proc. Natl. Acad. Sci. U.S.A. 100*, 15543−15547.
5. Lányi, J. K. (2004) Bacteriorhodopsin, *Annu. Rev. Physiol. 66*, 665−688.
6. Hunte, C., Palsdottir, H., and Trumpower, B. L. (2003) Protonmotive pathways and mechanisms in the cytochrome bc_1 complex, *FEBS Lett. 545*, 39−46.
7. Mitchell, P. (1966) Chemiosmotic coupling in oxidative and photosynthetic phosphorylation, *Biol. Rev. Cambridge Philos. Soc. 41*, 445−502.
8. Seelert, H., Poetsch, A., Dencher, N. A., Engel, A., Stahlberg, H., and Müller, D. J. (2000) Proton-powered turbine of a plant motor, *Nature 405*, 418−419.
9. Stowell, M. H. B., McPhillips, T. M., Rees, D. C., Soltis, S. M., Abresch, E., and Feher, G. (1997) Light-induced structural changes in photosynthetic reaction center: Implications for mechanism of electron-proton transfer, *Science 276*, 812−816.
10. Debus, R. J., Feher, G., and Okamura, M. Y. (1985) LM complex of reaction centers from *Rhodobacter sphaeroides* R-26: Characterization and reconstitution with the H subunit, *Biochemistry 24*, 2488−2500.
11. Hermes, S., Bremm, O., Garczarek, F., Derrien, V., Liebisch, P., Loja, P., Sebban, P., Gerwert, K., and Haumann, M. (2006) A time-resolved iron-specific X-ray absorption experiment yields no evidence for an $Fe^{2+} \rightarrow Fe^{3+}$ transition during $Q_A^- \rightarrow Q_B$ electron transfer in the photosynthetic reaction center, *Biochemistry 45*, 353−359.
12. Zhu, Z., and Gunner, M. R. (2005) The energetics of quinone dependent electron and proton transfers in *Rhodobacter sphaeroides* photosynthetic reaction centers, *Biochemistry 44*, 82−96.
13. Diner, B. A., Schenck, C. C., and DeVitry, C. (1984) Effect of inhibitors, redox state, and isoprenoid chain length on the affinity of ubiquinone for the secondary acceptor binding site in the reaction centers of photosynthetic bacteria, *Biochim. Biophys. Acta 766*, 9−20.
14. Wraight, C. A., and Shopes, R. J. (1989) Quinone binding and herbicide activity in the acceptor quinone complex of bacterial reaction centres, in *Techniques and New Developments in Photosynthesis Research* (Barber, J., and Malkin, R., Eds.) pp 183−191, Plenum Press, New York.
15. Graige, M. S., Paddock, M. L., Bruce, J. M., Feher, G., and Okamura, M. Y. (1996) Mechanism of proton-coupled electron transfer for quinone (Q_B) reduction in reaction centers of *Rb. sphaeroides*, *J. Am. Chem. Soc. 118*, 9005−9016.
16. McPherson, P. H., Okamura, M. Y., and Feher, G. (1990) Electron transfer from the reaction center of *Rb. sphaeroides* to the quinone pool: Doubly reduced Q_B leaves the reaction center, *Biochim. Biophys. Acta 1016*, 289−292.
17. Kleinfeld, D., Abresch, E. C., Okamura, M. Y., and Feher, G. (1984) Damping of oscillations in the semiquinone absorption in reaction centers after successive flashes: Determination of the equilibrium between $Q_A^-Q_B$ and $Q_AQ_B^-$, *Biochim. Biophys. Acta 765*, 406−409.
18. Maróti, P., and Wraight, C. A. (1988) Flash-induced H^+ binding by bacterial reaction centers: Influences of the redox states of the acceptor quinones and primary donor, *Biochim. Biophys. Acta 934*, 329−347.
19. Paddock, M. L., Rongey, S. H., Abresch, E. C., Feher, G., and Okamura, M. Y. (1988) Reaction centers from three herbicide-resistant mutants of *Rhodobacter sphaeroides* 2.4.1: Sequence analysis and preliminary characterization, *Photosynth. Res. 17*, 75−96.
20. Osváth, Sz., and Maróti, P. (1997) Coupling of cytochrome and quinone turnovers in the photocycle of reaction centers from the photosynthetic bacterium *Rhodobacter sphaeroides*, *Biophys. J. 73*, 972−982.
21. Gerencsér, L., Laczkó, G., and Maróti, P. (1999) Unbinding of oxidized cytochrome *c* from photosynthetic reaction center of *Rhodobacter sphaeroides* is the bottleneck of fast turnover, *Biochemistry 38*, 16866−16875.
22. Utschig, L. M., Ohigashi, Y., Thurnauer, M. C., and Tiede, D. M. (1998) A new metal binding site in photosynthetic bacterial reaction centers that modulates Q_A to Q_B electron transfer, *Biochemistry 37*, 8278−8281.
23. Paddock, M. L., Graige, M. S., Feher, G., and Okamura, M. Y. (1999) Identification of the proton pathway in bacterial reaction centers: Inhibition of proton transfer by binding of Zn^{2+} or Cd^{2+}, *Proc. Natl. Acad. Sci. U.S.A. 96*, 6183−6188.
24. Axelrod, H. L., Abresch, E. C., Paddock, M. L., Feher, G., and Okamura, M. Y. (2000) Determination of the binding sites of the proton transfer inhibitors Cd^{2+} and Zn^{2+} in bacterial reaction centers, *Proc. Natl. Acad. Sci. U.S.A. 97*, 1542−1547.
25. Gerencsér, L., and Maróti, P. (2001) Retardation of proton transfer caused by binding of the transition metal ion to bacterial reaction centers is due to pK_a shifts of key protonatable residues, *Biochemistry 40*, 1850−1860.
26. Gerencsér, L., and Maróti, P. (2004) Anomalous acceleration of the photocycle in photosynthetic reaction centers inhibited on the acceptor side, *Biopolymers 74*, 96−92.
27. Rosen, D., Okamura, M. Y., and Feher, G. (1980) Interaction of cytochrome *c* with reaction centers of *Rhodopseudomonas sphaeroides* R-26: Determination of number of binding sites and dissociation constants by equilibrium dialysis, *Biochemistry 19*, 5687−5692.
28. Van Gelder, B. F., and Slater, E. C. (1962) The extinction coefficient of cytochrome *c*, *Biochim. Biophys. Acta 58*, 593−595.
29. Stein, R. R, Castellvi, A. L., Bogacz, J. P., and Wraight, C. A. (1984) Herbicide-quinone competition in the acceptor complex of photosynthetic reaction centers from *Rhodopseudomonas sphaeroides*. A bacterial model for PSII-herbicide activity in plants, *J. Cell. Biochem. 24*, 243−259.
30. Lavergne, J., Matthews, C., and Ginet, N. (1999) Electron and proton transfer on the acceptor side on the reaction center in chromatophores of *Rhodobacter capsulatus*: Evidence for direct protonation of the semiquinone state of Q_B, *Biochemistry 38*, 4542−4552.
31. Osváth, Sz., Laczkó, G., Sebban, P., and Maróti, P. (1996) Electron transfer in reaction centers of *Rhodobacter sphaeroides* and *Rhodobacter capsulatus* monitored by fluorescence of the bacteriochlorophyll dimer, *Photosynth. Res. 47*, 41−49.
32. Maróti, P., and Wraight, C. A. (1997) Kinetics of H^+-ion binding by the $P^+Q_A^-$ state of the bacterial photosynthetic reaction centers: Rate limitation within the protein, *Biophys. J. 73*, 367−381.
33. Beauchamp, C., and Fridovich, I. (1971) Superoxide dismutase: Improved assays and an assay applicable to acrylamide gels, *Anal. Biochem. 44*, 276−287.
34. McCord, J. M., and Fridovich, I. (1969) Superoxide dismutase: An enzymatic function for erythrocuprein (hemocuprein), *J. Biol. Chem. 244*, 6049−6056.
35. Murphy, T. M., Vu, H., and Nguyen, T. (1998) The superoxide synthases of rose cells, *Plant Physiol. 117*, 1301−1305.

36. Alegria, A. E., Cordones, E., Santiago, G., Marcano, Y., Sanchez, S., Gordaliza, M., and Martín-Martín, M. L. (2002) Reductive activation of terpenylnaphthoquinones, *Toxicology 175*, 167−175.
37. Ädelroth, P., Paddock, M. L., Sagle, L. B., Feher, G., and Okamura, M. Y. (2000) Identification of the proton pathway in bacterial reaction centers: Both protons associated with reduction of Q_B to Q_BH_2 share a common entry point, *Proc. Natl. Acad. Sci. U.S.A. 97*, 13086−13091.
38. Okamura, M. Y., Debus, R. J., Kleinfeld, D., and Feher, G. (1982) Quinone binding site in reaction centers from photosynthetic bacteria, in *Function of Quinones in Energy Conserving Systems* (Trumpower, B. L., Ed.) pp 299−317, Academic Press, New York.
39. Keller, S., Beatty, J. T., Paddock, M. L., Breton, J., and Leibl, W. (2001) Effect of metal binding on electrogenic proton-transfer associated with reduction of the secondary electron acceptor (Q_B) in *Rhodobacter sphaeroides* chromatophores, *Biochemistry 40*, 429−439.
40. Ginet, N., and Lavergne, J. (2000) Interaction between the donor and acceptor sides in bacterial reaction centers, *Biochemistry 39*, 16252−16262.
41. Morrison, L. E., Schelhorn, J. E., Cotton, T. M., Bering, C. L., and Loach, P. A. (1982) Electrochemical and spectral properties of ubiquinone and synthetic analogs: Relevance to bacterial photosynthesis, in *Function of Quinones in Energy Conserving Systems* (Trumpower, B. L., Ed.) pp 35−58, Academic Press, New York.
42. Okamura, M. Y., Isaacson, R. A., and Feher, G. (1979) Spectroscopic and kinetic properties of the transient intermediate acceptor in reaction centers of *Rhodopseudomomas sphaeroides*, *Biochim. Biophys. Acta 546*, 394−417.
43. Maróti, P., Kirmaier, C., Holten, D., and Wraight, C. A. (1985) Photochemistry and electron-transfer in borohydride-treated photosynthetic reaction centers, *Biochim. Biophys. Acta 810*, 132−139.
44. Calvo, R., Abresch, E. C., Bittl, R., Feher, G., Hofbauer, W., Isaacson, R. A., Lubitz, W., Okamura, M. Y., and Paddock, M. L. (2000) EPR study of the molecular and electronic structure of the semiquinone biradical $Q_A^-Q_B^-$ in photosynthetic reaction centers from *Rhodobacter sphaeroides*, *J. Am. Chem. Soc. 122*, 7327−7341.
45. Nabedryk, E., Breton, J., Okamura, M. Y., and Paddock, M. L. (2005) Semiquinone (Q_B^-) interactions and protein structural changes in photosynthetic reaction center mutants at Asp-L213 and Glu-L212 sites, in *Photosynthesis: Fundamental Aspects to Global Perspectives* (van der Est, A., and Bruce, D., Eds.) Sect. V, pp 192−194, International Society of Photosynthesis.
46. Packham, N. K., Müller, P., and Dutton, P. L. (1988) Photoelectric currents across planar bilayer membranes containing bacterial reaction centers: The response under conditions of multiple reaction-center turnovers, *Biochim. Biophys. Acta 933*, 70−84.
47. Knox, P. P., Lukashev, E. P., Timofeev, K. N., and Seifullina, N. K. (2002) Effects of oxygen on the dark recombination between photoreduced secondary quinones and oxidized bacteriochlorophyll in *Rhodobacter sphaeroides* reaction centers, *Biochemistry (Moscow) 67*, 1085−1092.
48. Lancaster, C. R. D. (1998) Ubiquinone reduction and protonation in photosynthetic reaction centers from *Rhodopseudomonas viridis*: X-ray structures and their functional implications, *Biochim. Biophys. Acta 1365*, 143−150.
49. Taly, A., Sebban, P., Smith, J. C., and Ullmann, G. M. (2003) The position of Q_B in the photosynthetic reaction center depends on pH: A theoretical analysis of the proton uptake upon Q_B reduction, *Biophys. J. 84*, 2090−2098.
50. Pokkuluri, P. R., Laible, P. D., Crawford, A. E., Mayfield, J. F., Yousef, M. A., Ginell, S. L., Hanson, D. K., and Schiffer, M. (2004) Temperature and cryoprotectant influence secondary quinone binding position in bacterial reaction centers, *FEBS Lett. 570*, 171−174.
51. Land, E. J., and Swallow, A. J. (1970) One-electron reactions in biochemical systems as studied by pulse radiolysis, *J. Biol. Chem. 245*, 1890−1894.
52. Patel, K. B., and Willson, R. L. (1973) Semiquinone free radicals and oxygen: Pulse radiolysis study of one electron transfer equilibrium, *J. Chem. Soc. (Faraday I) 69*, 814−825.
53. Graige, M. S., Paddock, M. L., Feher, G., and Okamura, M. Y. (1999) Observation of the protonated semiquinone intermediate in isolated reaction centers from *Rhodobacter sphaeroides*: Implications for the mechanism of electron and proton transfer in proteins, *Biochemistry 38*, 11465−11473.
54. Swallow, A. J. (1982) Physical chemistry of semiquinones, in *Function of Quinones in Energy Conserving* Systems (Trumpower, B. L., Ed.) pp 59−72, Academic Press, New York.
55. Wood P. M. (1974) The redox potential of the system oxygen-superoxide, *FEBS Lett. 44*, 22−24.
56. Rich, P. R., and Bendall, D. S. (1980) The kinetics and thermodynamics of the reduction of cytochrome *c* by substituted *p*-benzoquinols in solution, *Biochim. Biophys. Acta 592*, 506−518.
57. Lancaster, C. R. D., Michel, H., Honig, B., and Gunner, M. R. (1996) Calculated coupling of electron and proton transfer in the photosynthetic reaction center of *Rhodopseudomonas viridis*, *Biophys. J. 70*, 2469−2492.
58. Okamura, M. Y., Paddock, M. L., Graige, M. S., and Feher, G. (2000) Proton and electron transfer in bacterial reaction centers, *Biochim. Biophys. Acta 1458*, 148−163.
59. Milano, F., Agostiano, A., Mavelli, F., and Trotta, M. (2003) Kinetics of the quinone binding reaction at the Q_B site of reaction centers from the purple bacteria *Rhodobacter sphaeroides* reconstituted in liposomes, *Eur. J. Biochem. 270*, 4595−4605.
60. McComb, J. C., Stein, R. R., and Wraight, C. A. (1990) Investigations on the influence of headgroup substitution and isoprene side-chain length in the function of primary and secondary quinones of bacterial reaction centers, *Biochim. Biophys. Acta 1015*, 156−171.
61. Madeo, J., and Gunner, M. R. (2005) Modeling binding kinetics at the Q_A site in bacterial reaction centers, *Biochemistry 44*, 10994−11004.
62. Gerencsér, L., Rinyu, L., Kálmán, L., Takahashi, E., Wraight, C. A., and Maróti, P. (2004) Competitive binding of quinone and antibiotic stigmatellin to reaction centers of photosynthetic bacteria, *Acta Biol. (Szeged) 48*, 25−33.
63. Ginet, N., and Lavergne, J. (2001) Equilibrium and kinetic for the binding of inhibitors to the Q_B pocket in bacterial chromatophores: Dependence on the state of Q_A, *Biochemistry 40*, 1812−1823.
64. Breton, J., Burie, J. R., Berthomieu, C., Berger, G., and Nabedryk, E. (1994) The binding sites of quinones in photosynthetic bacterial reaction centers investigated by light-induced FTIR difference spectroscopy: Assignment of the Q_A vibrations in *Rhodobacter sphaeroides* using ^{18}O- or ^{13}C-labeled ubiquinone and vitamin K_1, *Biochemistry 33*, 4953−4965.
65. Rutherford, A. W., and Evans, M. C. W. (1980) Direct measurement of the redox potential of the primary and secondary quinone electron acceptors in *Rhodopseudomonas sphaeroides* (wild type) by EPR spectrometry, *FEBS Lett. 110*, 257−261.
66. Wraight, C. A. (1981) Oxidation−reduction physical chemistry of the acceptor quinone complex in bacterial photosynthetic reaction centers: Evidence for a new model of herbicide activity, *Isr. J. Chem. 21*, 348−354.
67. Wraight, C. A. (1998) Functional linkage between the Q_A and Q_B sites of photosynthetic reaction centers, in *Photosynthesis: Mechanisms and Effects* (Garab, G., Ed.) pp 693−698, Kluwer Academic Publishers, Dordrecht, The Netherlands.
68. Ishikita, H., Morra, G., and Knapp, E. W. (2003) Redox potential of quinones in photosynthetic reaction centers from *Rhodobacter sphaeroides*: Dependence on protonation of Glu-L212 and Asp-L213, *Biochemistry 42*, 3882−3892.

BI052071M